

# Model-independent maximum-entropy method for the analysis of sum-frequency vibrational spectroscopy

Pao-Keng Yang and Jung Y. Huang

*Institute of Electro-Optical Engineering, Chiao Tung University, Hsinchu, Taiwan*

Received November 1, 1999; revised manuscript received March 2, 2000

We have developed and applied a maximum-entropy phase-retrieval procedure to analyze sum-frequency vibrational spectra from a  $\text{CCl}_4$ /octadecyl tricholasilane/silica interface and a hydrogen-terminated diamond C(111) surface. Some *a priori* knowledge of a nonlinear optical spectrum was employed for determining the phase of nonlinear optical susceptibility, and therefore the requirement for experimental phase measurement can be avoided. The results agree well with those from the Lorentzian line-shape model and justify the applicability of the *a priori* constraints employed in our phase-retrieval procedure. © 2000 Optical Society of America [S0740-3224(00)00907-3]

OCIS codes: 190.4350, 300.6490, 190.1900.

## 1. INTRODUCTION

Nonlinear optical spectroscopy provides valuable techniques for characterizing a variety of materials. With resonant excitations, the nonlinear optical (NLO) responses from materials can be enhanced, and the resulting NLO susceptibilities are described with a combination of a constant background and some resonant terms. To deduce the complex NLO susceptibility from an observed spectrum, a fit of the measured spectrum to a theoretical model with Lorentzian line shapes is employed. Inhomogeneous broadenings from materials and finite laser bandwidth are therefore neglected.

Recently, a phase-retrieval procedure based on the maximum-entropy principle has been proposed by Vartiainen *et al.*<sup>1-4</sup> and Peiponen.<sup>5,6</sup> The maximum-entropy phase-retrieval procedure (MEPRP) is superior to that based on the Kramers–Kronig relations<sup>7,8</sup> in two aspects. First, the MEPRP is applicable to degenerate cases<sup>3</sup> such as second-harmonic generation and degenerate four-wave mixing, for which the Kramers–Kronig relations do not hold. Second, the MEPRP needs only data interpolation, while the Kramers–Kronig relations require data extrapolation beyond the measured range. Applications of the MEPRP to third-harmonic generation spectroscopy<sup>3</sup> and infrared-visible sum-frequency generation (IVSFG) spectroscopy<sup>9</sup> had recently been demonstrated. However, in these studies at least one phase value must be known. This phase information is usually obtained from an interferometric measurement.<sup>10,11</sup> In this paper a maximum-entropy approach with some *a priori* knowledge of NLO susceptibility is developed for the analysis of IVSFG spectrum. Our method does not require any need for experimental phase measurements.

It is important to point out that both the modulus and phase of NLO susceptibility are required to depict the intrinsic NLO response of material fully. The MEPRP offers an objective and model-independent procedure for the

deduction of the NLO susceptibility from its measured modulus. In this paper we propose a method to separate the NLO susceptibility into the nonresonant and resonant parts. This was achieved without invoking any model for the resonant part. Note that a material response can be related to the Fourier transform of the resonant susceptibility. Direct curve fitting to the observed susceptibility modulus with a Lorentzian line-shape model implies that the material response be exponential decay. This is not true for many vibrational modes on a surface on which complicated couplings between adsorbates and substrate could exist.

This paper is organized as follows. In Section 2 we first briefly review the theoretical background of infrared-visible sum-frequency vibrational spectroscopy and the MEPRP. Some *a priori* knowledge of the NLO susceptibility is then proposed in Section 2(C) for the retrieval of its phase without experimental measurement. Some practical examples of the MEPRP are presented in Section 3. Finally, our conclusion is drawn in Section 4.

## 2. THEORETICAL BACKGROUND

### A. Theory of Infrared-Visible Sum-Frequency Generation

IVSFG is a second-order NLO process in which an infrared beam at frequency  $\omega_{\text{ir}}$  and a visible beam at frequency  $\omega_{\text{vis}}$  overlap in a medium and generate an output at the sum frequency  $\omega_s = \omega_{\text{vis}} + \omega_{\text{ir}}$ .<sup>12</sup> In the electric dipole approximation the nonlinear polarization  $P_i(\omega_s)$  induced by incident laser fields can be written as

$$P_i(\omega_s) = \chi_{ijk}^{(2)} E_j(\omega_{\text{vis}}) E_k(\omega_{\text{ir}}). \quad (1)$$

By symmetry, sum-frequency generation (SFG) is forbidden in media with an inversion center but is necessarily allowed at a surface or interface and therefore can be used to probe surfaces and interfaces. A sum-frequency

signal is proportional to the absolute square of the effective surface susceptibility  $\chi_s^{(2)}$ . Pronounced resonance in  $\chi_s^{(2)}$  can be observed if  $\omega_{\text{ir}}$  scans over a surface vibrational mode. In general, the signal can be described by<sup>12,13</sup>

$$I(\omega_s) \propto |\chi_s^{(2)}(-\omega_s; \omega_{\text{vis}}, \omega_{\text{ir}})|^2 \\ = |\chi_{\text{NR}}^{(2)} + \chi_{\text{R}}^{(2)}| = \left| \chi_{\text{NR}}^{(2)} + \sum_q \frac{A_q}{(\omega_{\text{ir}} - \omega_q + i\gamma_q)} \right|^2, \quad (2)$$

where  $\chi_{\text{NR}}^{(2)}$  is the nonresonant background and  $A_q$ ,  $\omega_q$ , and  $\gamma_q$  denote the resonant amplitude, frequency, and damping constant of the  $q$ th resonant mode. These parameters can be determined from the fit of a measured spectrum to Eq. (2). To facilitate further discussion, we shall call this data analysis scheme the Lorentzian line-shape model.

Like coherent anti-Stokes Raman scattering, the line shape of IVSFG is affected by an interference between the nonresonant part  $\chi_{\text{NR}}^{(2)}$  and the resonant part  $\chi_{\text{R}}^{(2)}$ .<sup>12,14</sup> Note that part of the nonresonant term is originated from substrate and could therefore be influenced by the surface structure of substrate. In some cases, such as C—H stretch on diamond substrates,<sup>15</sup>  $\chi_{\text{NR}}^{(2)}$  becomes complex with

$$\chi_{\text{NR}}^{(2)} = |\chi_{\text{NR}}^{(2)}| \exp(i\theta). \quad (3)$$

Separation of the nonresonant part from the resonant part is important and is usually achieved with a direct curve fitting by use of the Lorentzian line-shape model. In this paper we shall demonstrate an alternative method with which the complex nonresonant susceptibility can be extracted without invoking any model for the resonant part.

The superiority of the MEPRP to the Lorentzian model can be appreciated with the following two viewpoints. First, the MEPRP is model independent. Although a set of characteristic parameters can be determined from a fit to Eq. (2) by neglecting the inhomogeneous broadening effects, this determination is not generally correct. Indeed, IVSFG from silver substrate had revealed that the inhomogeneous broadening is not negligible.<sup>16</sup> We had shown in our previous study that the inhomogeneous broadening effects do not affect the error-phase behavior<sup>9</sup> and therefore can be easily incorporated into the MEPRP. Second, the MEPRP is the only technique for solving the phase-retrieval problem in NLO spectroscopy with transform-limited light pulses. This is important because transform-limited light pulses are most efficient for yielding a NLO signal under a given pulse energy and spectral resolution. However, to deduce the intrinsic response of material from an observed spectrum, a deconvolution technique must be employed for the removal of the line broadening from a finite laser bandwidth. As far as we know, the phase-retrieval problem in the deconvolution of coherent NLO spectroscopy can be solved only with the MEPRP.<sup>17</sup>

## B. Maximum-Entropy Phase-Retrieval Procedure

The entropy for a power spectrum  $S(f)$  in the frequency interval  $[f_1, f_2]$  is defined as

$$h \propto \int_{f_1}^{f_2} \log S(f) df. \quad (4)$$

We can introduce a normalized frequency  $\nu = (f - f_1)/(f_2 - f_1)$  to project the frequency interval from  $[f_1, f_2]$  onto  $[0, 1]$ . The variational calculus with the LaGrange multiplier method can find the solution that maximizes the spectral entropy defined by Eq. (4) with constraint of the autocorrelation function calculated from the measured spectral points. The resulting solution for  $2M + 1$  spectral points is

$$S(\nu) = \frac{|\beta|^2}{\left| 1 + \sum_{k=1}^M a_k \exp(i2\pi k\nu) \right|^2}, \quad (5)$$

where the coefficients  $a_k$ ,  $|\beta|^2$  can be determined from a Toeplitz system:

$$\begin{bmatrix} R(0) & R(-1) & \cdots & R(-M) \\ R(1) & R(0) & \cdots & R(1-M) \\ \vdots & \vdots & \ddots & \vdots \\ R(M) & R(M-1) & \cdots & R(0) \end{bmatrix} \begin{bmatrix} 1 \\ a_1 \\ \vdots \\ a_M \end{bmatrix} = \begin{bmatrix} |\beta|^2 \\ 0 \\ \vdots \\ 0 \end{bmatrix}. \quad (6)$$

Here  $R(m)$  is the autocorrelation function, which is the Fourier transform of power spectrum  $S(\nu)$ :

$$R(m) = \int_0^1 S(\nu) \exp(-i2\pi m\nu) d\nu. \quad (7)$$

Van den Bos had shown that the solution from the maximum entropy is an autoregressive process,<sup>18</sup> which is defined to be an observation  $x_m$  that is a linear combination of  $M$  preceding observations:

$$x_m = -\sum_{k=1}^M a_k x_{m-k} + e_m. \quad (8)$$

The error  $e_m$  is a zero-mean random variable, and the  $a_k$  denotes the same coefficients as those in Eq. (5).

Let the  $z$  transform of  $f_n$  and  $f_{n-i}$  be  $F(z)$  and  $z^{-i}F(z)$ , so that the  $z$  transform of Eq. (8) becomes

$$X(z) = -(a_1 z^{-1} + a_2 z^{-2} + \cdots + a_M z^{-M})X(z) + E(z). \quad (9)$$

If we set  $z = \exp(-i2\pi\nu)$ , the  $z$  transforms can readily be recognized as the discrete-time Fourier transforms.<sup>19</sup> Thus an expression for the complex spectral response can be found to be

$$X(\nu) = \frac{E(\nu)}{1 + \sum_{k=1}^M a_k \exp(-i2\pi k\nu)}. \quad (10)$$

If we further express the error spectrum as

$$E(\nu) = |\beta| \exp[i\phi(\nu)], \quad (11)$$

where  $\phi(\nu)$  denotes an error phase, then the maximum-entropy solution of  $\chi^{(2)}(\nu)$  can be found to be

$$\chi^{(2)}(\nu) = \frac{|\beta| \exp[i\phi(\nu)]}{1 + \sum_{k=1}^M a_k \exp(i2\pi k\nu)}. \quad (12)$$

Note that the coefficients  $a_k$ ,  $|\beta|^2$  can be deduced from Eq. (6), and the error phase  $\phi(\nu)$  in Eq. (12) becomes the only quantity that cannot be determined from the power spectrum  $S(\nu)$ . However, there exists a one-to-one correspondence between the error phase and the real phase  $\arg[\chi^{(2)}(\nu)]$ . The problem in the MEPRP is therefore simplified to find the corresponding error phase.

To discover a reasonable estimate of  $\phi(\nu)$ , we need additional information from the measured spectrum. For example, if we know the phase of NLO susceptibility at  $L + 1$  discrete frequencies, we can then compute the corresponding error phase and interpolate with a polynomial:

$$\phi(\nu) = B_0 + B_1\nu + \dots + B_L\nu^L = \sum_{l=0}^L B_l\nu^l. \quad (13)$$

Here  $B_l$  satisfies a Vandermonde system as

$$\begin{bmatrix} 1 & \nu_0 & \cdots & \nu_0^L \\ 1 & \nu_1 & \cdots & \nu_1^L \\ \vdots & \vdots & \ddots & \vdots \\ 1 & \nu_L & \cdots & \nu_L^L \end{bmatrix} \begin{bmatrix} B_0 \\ B_1 \\ \vdots \\ B_L \end{bmatrix} = \begin{bmatrix} \phi(\nu_0) \\ \phi(\nu_1) \\ \vdots \\ \phi(\nu_L) \end{bmatrix}. \quad (14)$$

It has been shown that  $\phi(\nu)$  is fairly smooth<sup>1,3</sup>; therefore, a linear interpolation from two known error-phase values  $\phi(\nu_1)$  and  $\phi(\nu_2)$  offers a good estimate. If more phase values are known, a better estimate can always be obtained with a higher-order polynomial interpolation.

In the MEPRP the linearity of error phase can be enhanced with a frequency-squeezing procedure.<sup>1,3</sup> For a spectrum with a finite range  $\omega \in [\omega_1, \omega_2]$ , the corresponding squeezed spectrum, which is characterized by a squeezing parameter  $K$ , is given by

$$|\chi_K^{(2)}(\nu)| \equiv \begin{cases} |\chi^{(2)}(\omega_1)| & 0 \leq \nu < \frac{K}{2K+1} \\ |\chi^{(2)}\{\omega_1 + (\omega_2 - \omega_1)[(2K+1)\nu - K]\}| & \frac{K}{2K+1} \leq \nu \leq \frac{K+1}{2K+1} \\ |\chi^{(2)}(\omega_2)| & \frac{K+1}{2K+1} < \nu \leq 1 \end{cases} \quad (15)$$

Thus by choosing  $K > 0$ , we effectively transform the spectrum into a narrower normalized frequency range.

### C. Some *a priori* Information for Phase Retrieval

The following three criteria from *a priori* information of NLO spectrum are proposed for retrieval of the error phase:

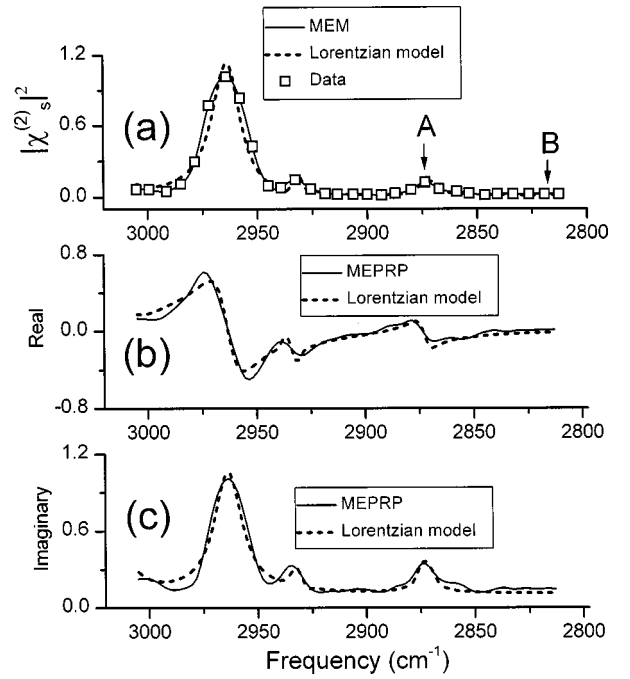


Fig. 1. Application of the phase-retrieval procedure in a SFG spectrum of OTS/CCl<sub>4</sub> interface. The solid curve in (a) denotes the maximum-entropy estimate. The real and imaginary parts obtained from the MEPRP are shown by the solid curves in (b) and (c). For comparison, the results from the Lorentzian line-shape model are presented with dashed curves.

**Criterion 1:** For a spectrum with an isolated peak and negligible background, the imaginary part of the NLO susceptibility has a peak position the same as that of the power spectrum.

**Criterion 2.** The real or the imaginary part of the NLO susceptibility should asymptotically approach a constant in a region far away from resonance.

**Criterion 3.** For an isolated peak, the imaginary part of the NLO susceptibility is an even function relative to the resonant frequency. Here the resonant frequency is determined from the peak position of the power spectrum.

Criterion 1 is justified, since for an isolated peak with

negligible background the imaginary part of the NLO susceptibility is symmetric while the real part is antisymmetric relative to the resonant frequency. The peak positions of the imaginary part therefore are the same as the peak position of the modulus. Criterion 2 is also valid because a NLO susceptibility in a region far away from resonance should be approximate to the nonreso-

nant background that behaves like a constant within the measured range. Criterion 2 provides two constraints on the error phase: one from the real part and the other from the imaginary part. It should be pointed out that the regions with asymptotic constant intensity, which are of no interest to most spectroscopic studies, become important in our analysis. Criterion 3 suggests that for a spectrum with nonoverlapping peaks the imaginary part of NLO susceptibility should be even, relative to each resonant frequency.

### 3. APPLICATIONS OF THE MAXIMUM-ENTROPY PHASE-RETRIEVAL PROCEDURE IN PRACTICAL INFRARED-VISIBLE SUM-FREQUENCY GENERATION SPECTRA

To demonstrate the usefulness of our method, we applied the MEPRP to analyze IVSFG spectra from two interfacial systems. The first example represents the case with multiple peaks and small background. The second system is chosen to demonstrate the applicability of the MEPRP in cases with significant complex background.

#### A. Infrared-Visible Sum-Frequency Generation Spectrum from $\text{CCl}_4/\text{OTS}/\text{Silica}$ Interface

In Fig. 1 the analysis of an IVSFG spectrum from a  $\text{CCl}_4/\text{octadecyl tricholasilane (OTS)}/\text{silica}$  interface<sup>14</sup> is presented to illustrate the detailed procedure of phase retrieval with *a priori* information. The squares denote the signal is proportional to the absolute square of the effective spectrum measured with a *p*-polarized visible beam at  $0.532 \mu\text{m}$  and a *p*-polarized infrared beam tunable  $\sim 3 \mu\text{m}$ . The solid curve in Fig. 1(a) denotes the maximum-entropy estimate with Eq. (5) for the observed spectrum.

In this analysis a continuous power spectrum  $S(\nu)$  was first prepared from the discrete measured points with a cubic spline interpolation. The continuous Fourier transform was then applied to deduce the autocorrelation function with Eq. (7). We used a frequency-squeezing procedure with  $K = 1$  to enhance the linearity of the error-phase function. The error phase was then approximated with a linear equation by  $\phi(\nu) = \phi_0 + \phi_1\nu$ . This is justified by our previous studies,<sup>9</sup> which indicated that the error phase can be well approximated with a linear interpolation as long as the nonresonant background is small.

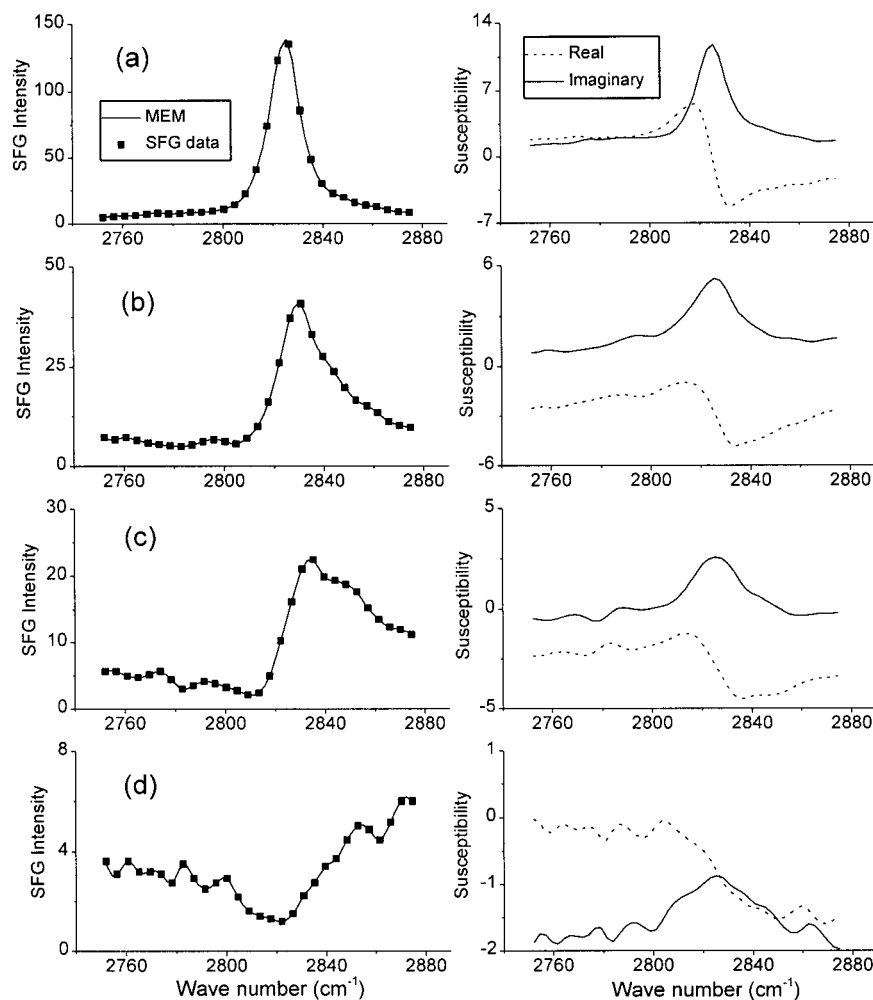


Fig. 2. Phase-retrieval results of IVSFG spectra of H/C(111) diamond ( $1 \times 1$ ) surfaces with different hydrogen coverages: (a) 100% monolayer (ML), (b) 49% ML, (c) 29% ML, and (d) 14% ML. The real and imaginary parts obtained from the MEPRP are shown on the right side. The error phase was approximated with a linear function of frequency.

Here the two unknown parameters  $\phi_0$  and  $\phi_1$  were determined by applying two constraints on the measured spectrum. These constraints include the applications of criterion 1 on the peak labeled A and criterion 2 on the position labeled B. The real and the imaginary parts obtained are shown with solid curves in Figs. 1(b) and 1(c). For comparison, the results from the Lorentzian line-shape model were also presented in Figs. 1(a), 1(b), and 1(c) with dashed curves. The slight discrepancy between the results from the Lorentzian line-shape model and the MEPRP can be attributed to the fact that Eq. (2) does not properly include the spectral broadening effects from laser linewidth<sup>17</sup> and inhomogeneous broadening.<sup>9</sup> This comparison also points out one merit of the MEPRP, i.e., the MEPRP is model independent; therefore, it could yield a more objective result.

### B. Infrared-Visible Sum-Frequency Generation Spectra from H/C(111) Surface with Varying Hydrogen Coverages

In Fig. 2 the MEPRP was applied to analyze IVSFG spectra from diamond C(111) surfaces with different hydrogen coverages. Four measured spectra (squares) are presented on the left side of the figure. The real (dashed curves) and the imaginary (solid curves) parts obtained from the MEPRP are shown on the right side.

Similar to the previous example, the error phase can be approximated by a linear function with frequency-squeezing procedure of  $K = 1$ . Two constraints were employed for deducing the coefficients in the linear error-phase function. We first applied criterion 1 to the spectrum shown in Fig. 2(a), where the nonresonant background is much smaller than the resonant peak. The constraint requires that the peak in the imaginary part to be at the same frequency as that of the modulus peak. Criterion 3, which demands that the imaginary part to be an even function relative to the resonant frequency, can then be applied. This constraint can be incorporated into the MEPRP by requiring the area on the left side of the peak to have the same value as that on the right side. The requirement is illustrated in Fig. 3. Here the frequency interval  $\Delta\nu$  used was chosen to be 0.2 in units of normalized frequency. The same procedure was also applied to Figs. 2(b), 2(c), and 2(d), where the resonant frequencies were chosen to be the same as that used in Fig. 2(a). Figure 4 presents the comparison between the analysis of the spectrum in Fig. 2(c) with the Lorentzian line-shape model (dashed curve) and that with the MEPRP (solid curve). The excellent agreement justifies the two criteria used in our phase-retrieval procedure.

From the retrieved imaginary and real parts, which were presented on the right side of Fig. 2, we can then deduce the real and imaginary parts of the nonresonant background. In view of the fact that on resonance the resonant susceptibility becomes purely imaginary, we first assign the real part of the nonresonant background to have the same value as the real part of the total NLO susceptibility at the resonant frequency. The imaginary part of  $\chi_{NR}^{(2)}$  can then be determined from the imaginary part of the total NLO susceptibility at a nonresonant position (i.e., the leftist position of the measured range). Note that the position should be chosen to be as far away

from resonances as possible, otherwise phase errors could arise. Nevertheless, the errors should be the same for all H/C(111) surfaces with different coverages. The real and imaginary parts of  $\chi_{NR}^{(2)}$  deduced from four spectra are shown in Fig. 5(a). The overall behavior is similar to that of Lorentzian line-shape model [see Fig. 5(b)].<sup>12</sup>

Deviation from linear dependence on surface coverage was found to occur at a coverage of  $\sim 30\%$ . This can be understood as follows. An ideal truncated surface of C(111) has a  $(1 \times 1)$  structure with one dangling bond for each exposed carbon atom. The sample prepared for the study started at a surface with all dangling bonds saturated by hydrogen atoms. We then partially release the dangling bonds from the hydrogen atoms by thermal desorption. The surface electronic structure of C(111)-(1  $\times$  1) with partial hydrogen coverage is not currently clear. Intuitively, we can expect that when the hydrogen coverage is below  $1/[1 + (6 \times 1/3)] = 1/3$  of full cover-

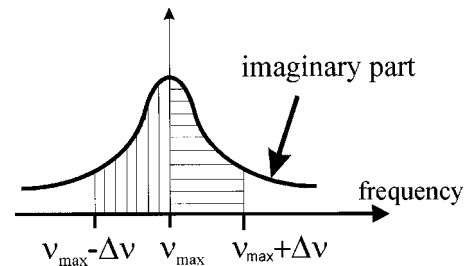


Fig. 3. Schematic diagram illustrating the constraint used in the phase retrieval of Fig. 2, which depicts the area marked by vertical lines to be equal to that marked by horizontal lines.

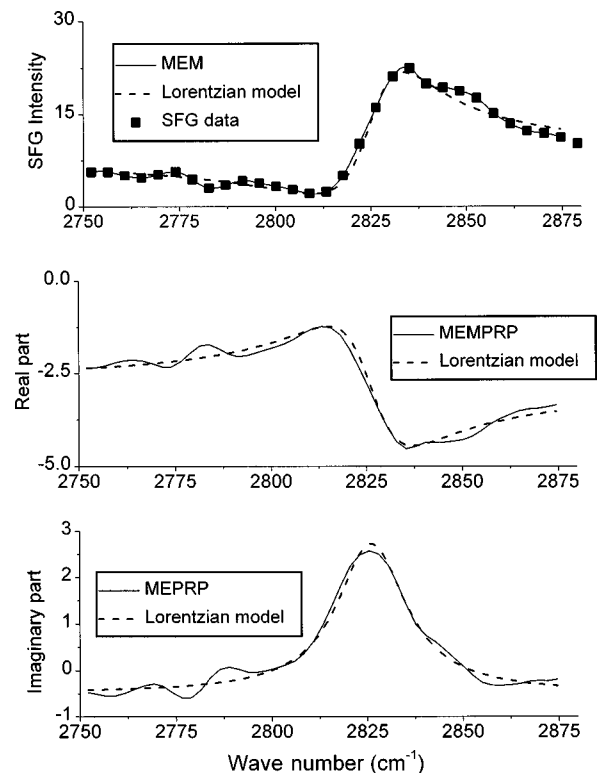


Fig. 4. Comparison of the results with the Lorentzian line-shape model (dashed curves) and the MEPRP (solid curves) for the spectrum shown in Fig. 2(c).

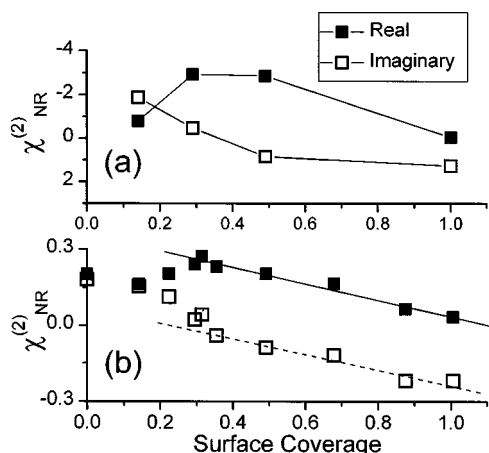


Fig. 5. Real and imaginary parts of nonresonant background as a function of surface hydrogen coverage ( $\Theta_H$ ) deduced with (a) the MEPRP and (b) the Lorentzian line-shape model. The solid curves in (a) are drawn for eye guiding, while the straight lines in (b) are a fit to  $A + B(1 - \Theta_H)$  for  $\Theta_H \geq 30\%$ .

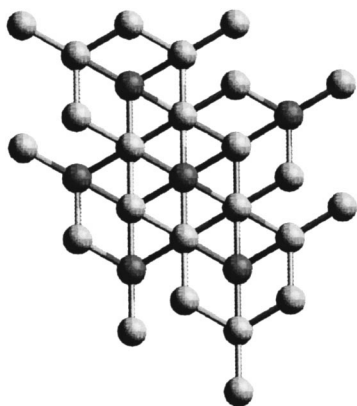


Fig. 6. Ball-and-stick model of the top view of C(111)-(1  $\times$  1) surface.

age (see Fig. 6), there is a high probability that the exposed carbon atoms with dangling bonds become nearest neighbors. Thus these dangling orbitals can overlap with each other to form the surface band gradually when the coverage is further decreased. The deviation of  $\chi_{NR}^{(2)}$  from the linear dependence of hydrogen coverage can therefore be ascribed to an appearance of the surface states in view of the fact that the sum-frequency photons generated are near the transition frequency from the valence band to the half-filled surface states.<sup>20</sup> As the coverage is larger than one-third, the dangling orbitals are isolated by the hydrogen-terminated carbon atoms and are able to preserve their electronic bonding nature. This leads to the observed linear dependence of  $\chi_{NR}^{(2)}$  at high surface coverage.

#### 4. CONCLUSION

We have applied the MEPRP procedure to analyze IVSFG spectra from various interface and surface. Some *a priori* knowledge from NLO spectra was used to estimate the error phase. The real and imaginary parts deduced from the MEPRP were found to agree with those from the

Lorentzian line-shape model, which justifies the constraints used in our MEPRP. The proposed IVSFG analysis procedure can yield a more objective picture for the system being studied.

#### ACKNOWLEDGMENTS

We acknowledge the financial support from the National Science Council of the Republic of China under grant NSC 88-2212-M-009-039. J. Y. Huang thanks the reviewers for bringing Ref. 19 to his attention.

J. Y. Huang, the corresponding author, can be reached at the address on the title page, by fax at 886-3-5716631, or by e-mail at jyhuang@cc.ntu.edu.tw.

#### REFERENCES

1. E. M. Vartiainen, "Phase retrieval approach for coherent anti-Stokes Raman scattering spectrum analysis," *J. Opt. Soc. Am. B* **9**, 1209–1214 (1992).
2. E. M. Vartiainen and K.-E. Peiponen, "Meromorphic degenerate nonlinear susceptibility: phase retrieval from the amplitude spectrum," *Phys. Rev. B* **50**, 1941–1944 (1994).
3. E. M. Vartiainen, K.-E. Peiponen, and H. Kishida, "Phase retrieval in nonlinear optical spectroscopy by the maximum-entropy method: an application to the  $|\chi^{(3)}|$  spectra of polysilane, T. Koda," *J. Opt. Soc. Am. B* **13**, 2106–2114 (1996).
4. E. M. Vartiainen, K.-E. Peiponen, and T. Asakura, "Phase retrieval in optical spectroscopy: resolving optical constants from power spectra," *Appl. Spectrosc.* **50**, 1283–1289 (1996).
5. K.-E. Peiponen, E. M. Vartiainen, and T. Asakura, "Dispersion theory and phase retrieval of meromorphic total susceptibility," *J. Phys.: Condens. Matter* **9**, 8937–8943 (1997).
6. K.-E. Peiponen, E. M. Vartiainen, and T. Asakura, "Dispersion theory of effective meromorphic nonlinear susceptibility of nanocomposites," *J. Phys.: Condens. Matter* **10**, 2483–2488 (1998).
7. F. L. Ridener and R. H. Good, "Dispersion relations for nonlinear systems of arbitrary degree," *Phys. Rev. B* **11**, 2768–2770 (1975).
8. H. Kishida, T. Hasegawa, Y. Iwasa, T. Koda, and Y. Tokura, "Dispersion relation in the third-order electric susceptibility for polysilane films," *Phys. Rev. Lett.* **70**, 3724–3727 (1993).
9. P.-K. Yang and J. Y. Huang, "Phase-retrieval problems in infrared-visible sum-frequency generation spectroscopy by the maximum-entropy method," *J. Opt. Soc. Am. B* **14**, 2443–2448 (1997).
10. R. Superfine, J. Y. Huang, and Y. R. Shen, "Phase measurement for surface infrared-visible sum-frequency generation," *Opt. Lett.* **15**, 1276–1278 (1990).
11. R. Superfine, J. Y. Huang, and Y. R. Shen, "Experimental determination of the sign of molecular dipole derivatives: an infrared-visible sum frequency generation absolute measurement study," *Chem. Phys. Lett.* **172**, 303–306 (1990).
12. J. Y. Huang and Y. R. Shen, "Sum-frequency as a surface probe," in *Laser Spectroscopy and Photochemistry on Metal Surfaces*, H. L. Dai and W. Ho, eds. (World Scientific, Singapore, 1995), Vol. 1, pp. 5–53.
13. S. H. Lin and A. A. Villaeys, "Theoretical description of steady-state sum-frequency generation in molecular adsorbates," *Phys. Rev. A* **50**, 5134–5144 (1994).
14. P. Guyot-Sionnest, R. Superfine, J. H. Hunt, and Y. R. Shen, "Vibrational spectroscopy of a silane monolayer at air/solid and liquid/solid interfaces using sum-frequency generation," *Chem. Phys. Lett.* **144**, 1–5 (1998).

15. R. P. Chin, J. Y. Huang, Y. R. Shen, T. J. Chuang, H. Seki, and M. Buck, "Vibrational spectra of hydrogen on diamond C(111)-(1 × 1)," *Phys. Rev. B* **45**, 1522–1524 (1992); R. P. Chin, J. Y. Huang, Y. R. Shen, T. J. Chuang, and H. Seki, "Interaction of atomic hydrogen with the diamond C(111) surface studied by infrared-visible sum-frequency generation spectroscopy," *Phys. Rev. B* **52**, 5985–5995 (1995).
16. T. H. Ong, P. B. Davies, and A. M. Creeth, "Polymer-surfactant aggregates at a hydrophobic surface studied using sum-frequency vibrational spectroscopy," *Langmuir* **11**, 2931–2937 (1995).
17. P.-K. Yang and J. Y. Huang, "Linewidth-deduction method for nonlinear optical spectroscopy with transform-limited light pulses," *J. Opt. Soc. Am. B* **15**, 1130–1134 (1998).
18. Van den Bos, "Alternative interpretation of maximum entropy spectral analysis," *IEEE Trans. Inf. Theory* **IT-17**, 493–494 (1971).
19. T. J. Ulrych and M. Ooe, "Autoregressive and mixed autoregressive-moving average models and spectra," in *Nonlinear Methods of Spectral Analysis*, S. Haykin, ed. (Springer-Verlag, Berlin, 1983), Chap. 3, pp. 73–125.
20. J. Ihm, S. G. Louie, and M. L. Cohen, "Self-consistent pseudopotential calculations for Ge and diamond (111) surfaces," *Phys. Rev. B* **17**, 769–775 (1978).